# DESIGN OF A 20 MeV PROTON LINEAR ACCELERATOR, NEW INJECTOR FOR SATURNE

M. Promé
C. E. N., Saclay

## Introduction

In order to increase the number of particles accelerated by the 3 BeV proton synchrotron SATURNE, it has been decided to replace its 3.6 MeV Van de Graaff injector by a 20 MeV linear accelerator.[1] This accelerator is now being built. My purpose is to present the main ideas which led to the design of this machine, and how the geometrical dimensions have been chosen.

## Requirements

The design of the machine proceeds logically from following parameters:

injection energy into the linac: 750 keV
normalized source emittance ($E\beta\gamma$): $\pi \cdot \frac{1}{\pi}$ mm.m.rad.
current intensity at the output of the linac: 20 mA
pulsed beam duration: 620 μs
energy spread after debunching: ± 48 keV, with occupation as homogeneous as possible in that energy range
output energy: linearly variable around 20 MeV during the beam pulse at the rate of 1 keV/μs.

This last requirement is somewhat unusual for a linear accelerator; it comes from the wish of injecting into the synchrotron without betatron oscillations. This can be achieved with an auxiliary cavity so-called "energy shifter"; this cavity has the same dimension as the debuncher, and is variable phase fed. We shall just point out that, on account of this device, it will be convenient to get a well bunched beam at the output of the accelerator.

One condition for the drift tubes size may be derived from the previous general requirements; the beam pulse duration leads to dc feed the windings of the quadrupoles; large drift tubes will then be needed to provide enough room for lodging the quadrupoles, at least at the beginning of the linac; a very suitable shape from this point of view is the shape proposed by Harwell: a cylindrical body with flat lids joined by quarters of circles. Moreover, this shape is rather easy to manufacture; it has been selected for this linac design.

The current intensity wished at the output of the accelerator is relatively small. However, experience acquired with other accelerators showed it is unwise to limit the maximum current available from a linear accelerator if one does not have serious reasons for doing it. This is why the first drift tubes holes have been chosen with a larger diameter than strictly useful; of course these first few cells will have a rather poor transit time factor, but they actually will not behave as a bottleneck.

## Computation Facilities

Computations have been carried on with two different programs written in Saclay. The first one IDDA, written by Mr. A. Katz computes elementary cell electrical properties, for a given geometry; the second one determines the drift tubes distribution along the machine, and then computes trajectories of sets of particles. Those two programs are related to the well-known MESSYMESH and PARMILA programs from MURA, from which several ideas have been borrowed.

IDDA can compute tubes made of a cylindrical body; a quarter of meridian consists of three straight sections joined by arcs of circle.

The figure taken for $\alpha = 0$ gives the tubes mentioned above, as well as the tubes that will be considered now.

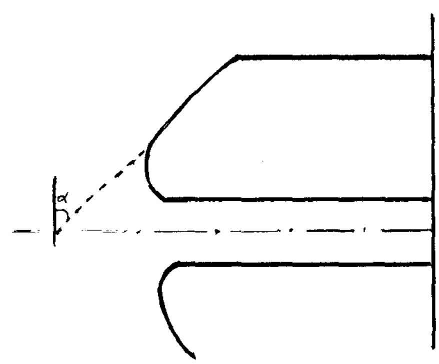


With a 8000 points mesh, results are obtained with a precision given by:

- error on f : 50 kc/s (including the error due to the fact that finite difference equations are considered instead of differential ones)
- error on T : 2 to 3%
- error on $E_m$ : 5%
- error on $Z_s$ : 1%

- f : resonance frequency
- T : transit time factor
- $E_m$: maximum electrical field
- $Z_s$: shunt impedance

The second program, which computes the drift tubes distribution can take into account a variable synchronous phase along the accelerator according to an arbitrary chosen law; the cell length is no more $\beta\lambda$, but this value corrected by the synchronous phase variation along the cell; moreover, computations take into account the corrective term $\frac{dT}{dW}$

which insures the phase area invariance; this point has been explained at the International Conference held in Frascati in 1965.[2]

Some precautions have been taken about the transit time factor; by entering into the program corrected values of the gap lengths, or of the bore diameter, one can simulate in this program transit time factor values in good agreement with the values given by the IDDA program.

Finally, cell lengths obtained with this program have been compared with the values given by a more sophisticated program written at C.E.R.N. by Dr. A. Carne; this later program uses the equations described in the quoted communication; its results, deemed better, have been adopted.

We are now going to explain how these programs have been used.

## Choice of the Main Dimensions

Figure 1 shows a general cell. Chosen frequency is 200 Mc/s; as it is impossible to choose a priori cells dimensions to get a given resonance frequency, each cell considered below results of a linear interpolation on g to get the nominal resonance frequency, other geometrical parameters being kept constant (figure 2). The field values are given for 1 MV/m average on the axis.

The first parameter to be chosen is the tank diameter, D. The selected value must be such that from .75 up to 20 MeV (L varying from 6 cm. up to 30 cm.) it leads to possible values of d and g (tube diameter and gap length) providing: maximum room for the quadrupoles; transit time factor T as high as possible; maximum field $E_m$ not too large.

Shunt impedance has little importance in this design, since the TH 515 tube is capable of a comfortable power for a 20 MeV accelerator.

$Z_s\ T^2$, $\frac{E_m}{T}$ and $\frac{g}{L}$ are significant parameters from the point of view of these criterions; hence comes the idea of looking at their variations around the D and d values usually chosen.

Figures 3, 4, and 5 show the situation for L = 6 cm, 22 cm. and 30 cm. A point on one of these figures represents a drift tube; the set of 3 values mentioned on the right side of the point gives $Z_s\ T^2$, $\frac{E_m}{T}$ and $\frac{g}{L}$ respectively. The field is normalized at 1 MV/m on the axis.

Comparison of figures 3 and 5 shows that a cavity diameter of 1 m. may be selected from the point of view of the criterions stated above; drift tubes diameter is then around 18 cm. at low energy and 15 cm. at high energy. Figure 4 verifies that drift tubes may be easily chosen in the middle of the accelerator with this 1 m. tank diameter.

Families of tubes ranging from 6 cm. cell length up to 30 cm. remained to be determined. Inside a given family g is function of L, the other geometrical parameters being kept constant; from one family to another one, at least one of these parameters varies. A family is valid for a certain range of L, limited on one side by the condition that the maximum field is smaller than 4.9 MV/m for 1 MV/m on the axis (this means 13 MV/m maximum field for nominal field on the axis), and limited on the other side by the fact that the transit time factor goes down for high g/L. The junction condition between two families is that the transit time factor must not drop more than 5 per cent.

After a few trials, 6 families have been chosen; figure 6 gives their geometrical parameters figure 7 displays functions $\frac{g}{L}$ (L), T (L), $E_m$(L) (normalized at 1 MV/m on the axis) for the 6 families.

While the free parameter has been, until now, the cell length L, the program I am going to talk about in the next paragraph, will more readily accept N, the cell number, as free parameter.

The two programs are connected by the set of g/L values; in the case where the second program accepts only $\frac{g}{L}$ (N) values as data, some iterations are needed to succeed in finding agreeable values of $\frac{g}{L}$.

## Particle Dynamics in the Accelerator

Electrical field is assigned to be constant on the axis; it might as well be assumed that the field varies along the axis according to an arbitrary law imposed by particular devices such as ball tuners.

Synchronous phase $\phi_s$ is a chosen variable along the accelerator; figure 8 shows its variation in function of cell number N. Having $\phi_s$ variable allows increasing longitudinal acceptance without significant increase of the accelerator length. Figure 9 shows the stable area in ($\Delta$W, $\phi$) space for $\phi_s = 45^\circ$ at the beginning of the machine; this area is roughly speaking double than the area one could get with $\phi_s = 30^\circ$; even if this available area is not entirely filled with particles, it is however interesting to point out that particles will be located in the center region which is almost linear. Keeping $\phi_s = 45^\circ$ constant would give too long a machine; but one can progressively decrease $\phi_s$ down to $25^\circ$ without losing longitudinal acceptance, since the stable area goes up with energy while the area occupied by the beam remains constant; field variations of a few percent are tolerable. One could even decrease $\phi_s$ down to $20^\circ$ instead of $25^\circ$; however the beam exhibits in this case a large extension in $\phi$ at the output; that is undesirable because of the energy shifter.

The accelerator designed in that way has 59 cells (58 drift tubes plus 2 half drift tubes); their lengths are given by figure 10. Total length is 10.48 m; electrical field on the axis is 2.7 MV/m; average acceleration rate is 1.88 MeV/m.

Half radial acceptances are displayed in figure 11 for particles coming in vertical plane and in figure 12 for particles coming in horizontal plane; numbers given in these figures are $\frac{1}{50}$ of capture efficiency; the ion source that will feed the accelerator has an emittance such that the beam will occupy regions of high efficiency, about 80 percent.

This rather high efficiency is a secondary consequence of using a double buncher; its main purpose being to insure a rather uniform occupancy of the longitudinal stability space; thanks to the coupling between longitudinal and radial motions, the outcoming beam exhibits a regular energy spectrum within a certain band; figure 13 shows the occupation in ($\Delta W$, $\phi$) space; the requirements stated above are then fulfilled after debunching.

References

1. J. Faure, M. Gouttefangeas, R. Levy Mandel, M. Prome, G. Rastoix, G. Rommel et R. Vienet, "A New Injector for the Saturne Synchrotron," Proceedings of the International Conference on High Energy Accelerators (Frascati, 1965).

2. A. Carne, P. Lapostolle, M. Promé, "Accurate Beam Dynamics Equations in Proton Linear Accelerators," Proceedings of the International Conference on High Energy Accelerators (Frascati 1965).

DISCUSSION

M. PROMÉ, Saclay

CORK, LRL: What intensity do you expect from Saturn?

PROMÉ: $3 \times 10^{12}$ accelerated particles/pulse.

SWENSON, LASL: How many stems and what configuration do you plan to use for the low-energy drift tubes?

PROMÉ: It will be a one-stem configuration.

SWENSON: Of what diameter?

PROMÉ: About 25 mm diameter. It will be made of steel with a copper covering.

SWENSON: Do you plan to have these stems in the verticle plane?

PROMÉ: Not exactly. They will have to be tilted at the beginning of the machine because there is not enough room for the heads of the stems.

FEATHERSTONE, Univ. of Minnesota: The configuration you have drawn is the one used in the old Bevatron injector and the present Minnesota tank one. Our drift tubes have rather pliable copper stems, and it is customary when we open this tank to see the center passage in the shape of two intersecting circles. I suggest that if you do this, you should have a rather stiff stainless-steel body encased within the outer copper structure on the stem. They droop.

ALLISON, LRL: Let me reinforce that comment. On the old Bevatron injector we had a telescope with which we could look down the bore. With this type of stem configuration it was a linear tank. You could see the drift tubes, and as you looked down the machine they zig-zagged. Misalignments are bad on a strong-focused linear accelerator. I think it is imperative that you adopt a very stiff stem configuration. On the 20-MeV machine, now installed, we use two stems. Where the drift tubes are close together, the stems alternate from side to side.

PROMÉ: Are these stems made of copper-clad stainless steel?

ALLISON: I think they are stainless steel which is copper clad.

CARNE, RHEL: I would like to add to the remarks of Bob Featherstone, that the Minnesota linac is built on the side of a railway embankment, and, as a train goes by, there are some very interesting modulation effects on the beam because of the vibration. The question I would like to ask is: I see that you are planning to accelerate a 20-mA beam in a tank on the order of 10 m long. Do you intend to take any steps for beam-loading compensation?

PROMÉ: Provisions have been taken in the design of the modulators so that beam-loading compensation could be done, but nothing has been decided to date.

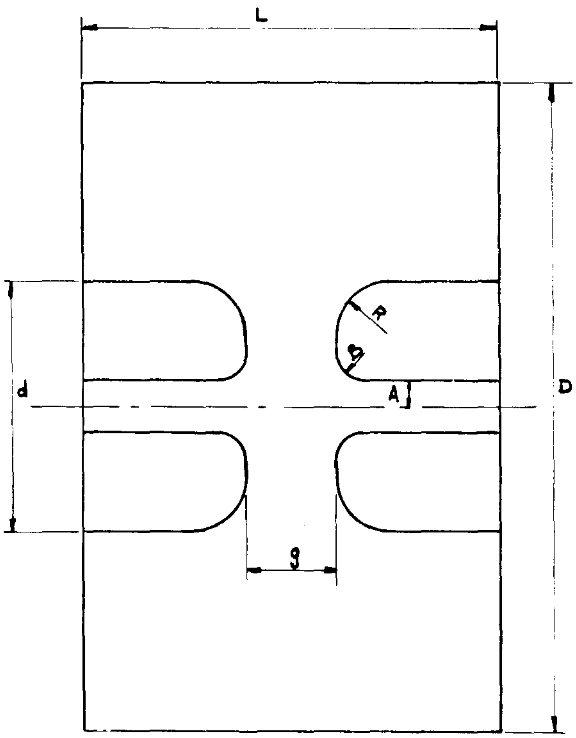


Figure 1.

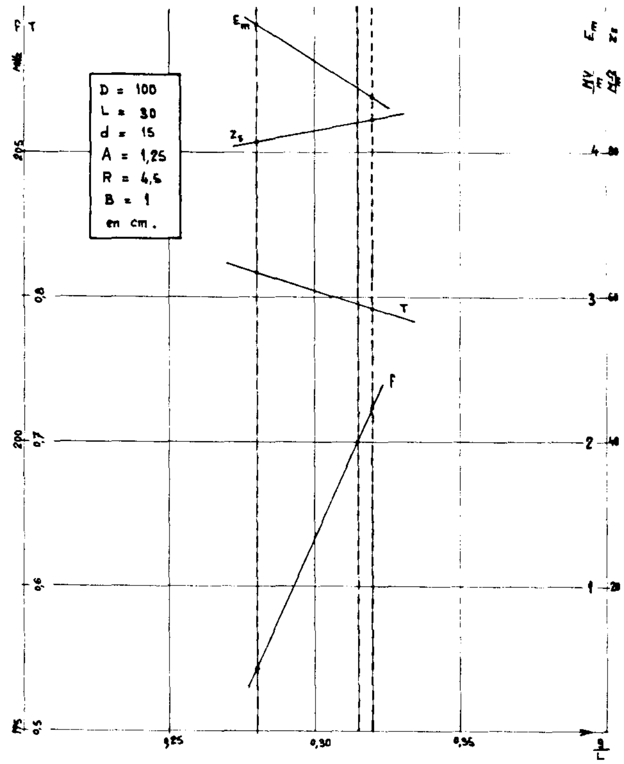


Figure 2.

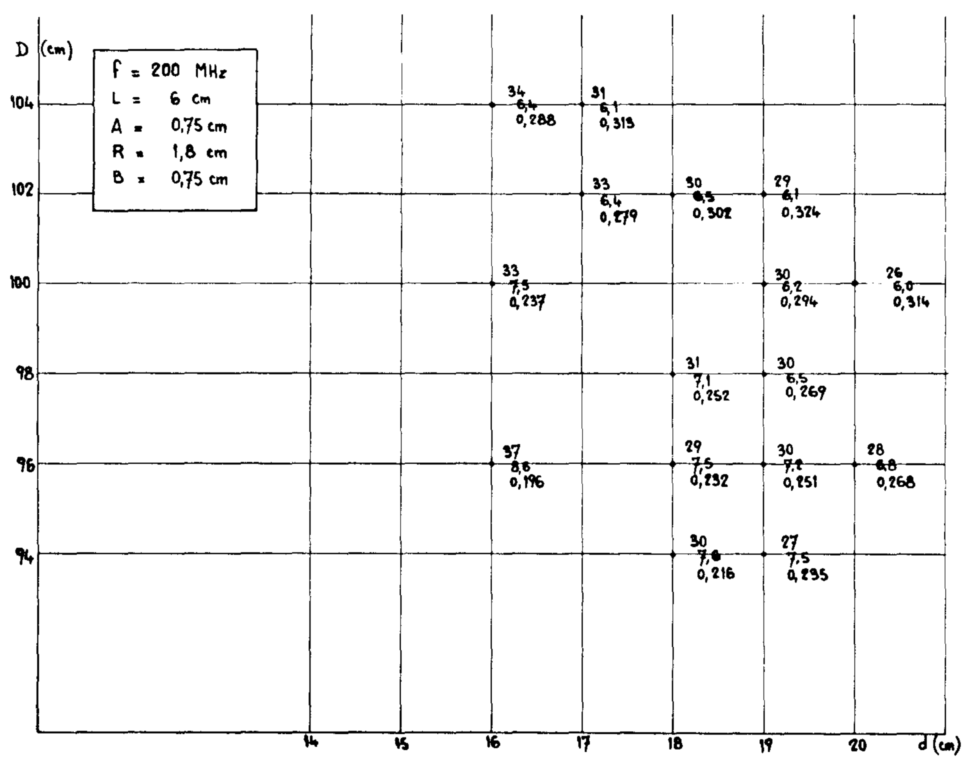


Figure 3.

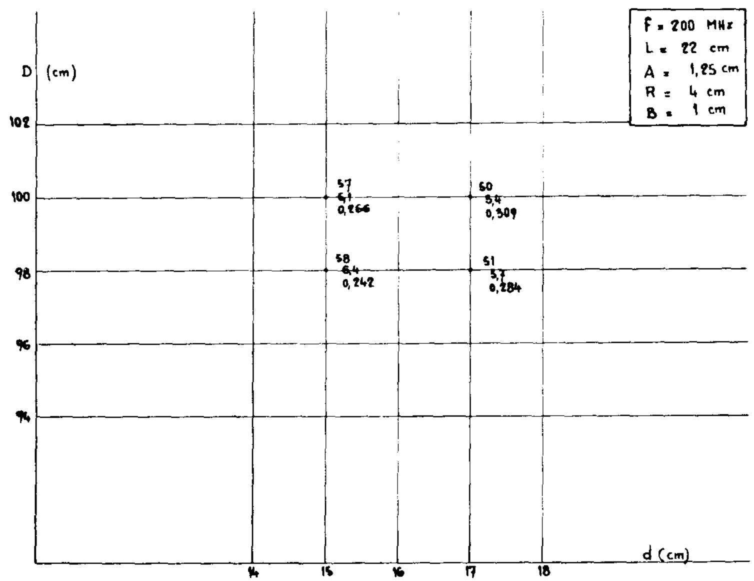


Figure 4.

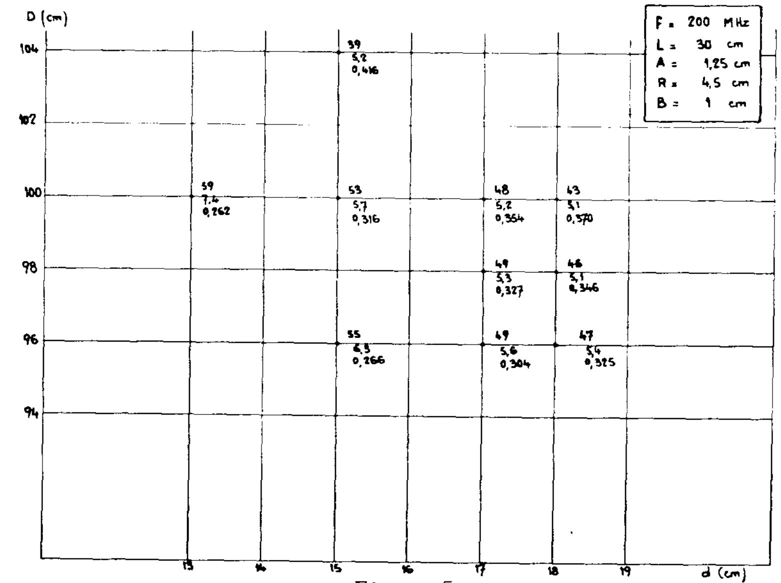


Figure 5.

| Familles | d | A | R | B | Limites de validité |
|---|---|---|---|---|---|
| 1 | 18 | 0,79 | 1,80 | 0,75 | L ≤ 9,2 |
| 2 | 18 | 0,92 | 2,50 | 0,75 | 9,2 < L ≤ 13,6 |
| 3 | 17 | 0,92 | 3,50 | 1,00 | 13,6 < L ≤ 16,7 |
| 4 | 16 | 1,07 | 3,50 | 1,00 | 16,7 < L ≤ 21,2 |
| 5 | 16 | 1,25 | 4,50 | 1,00 | 21,2 < L ≤ 25,2 |
| 6 | 15 | 1,25 | 4,50 | 1,00 | 25,2 < L |

Figure 6. *en centimetres*

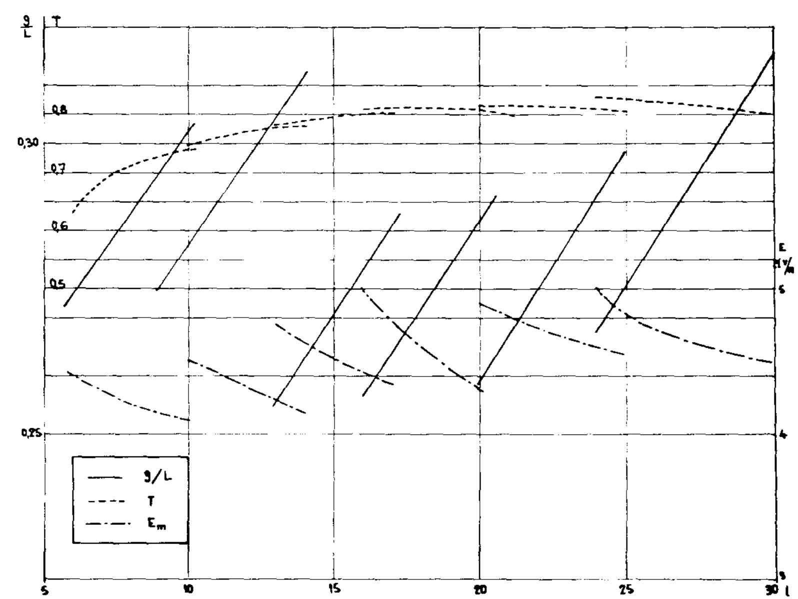


Figure 7.

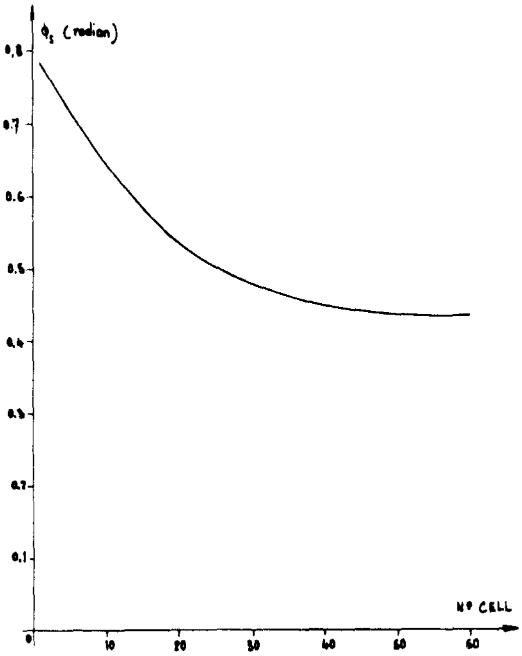


Figure 8.

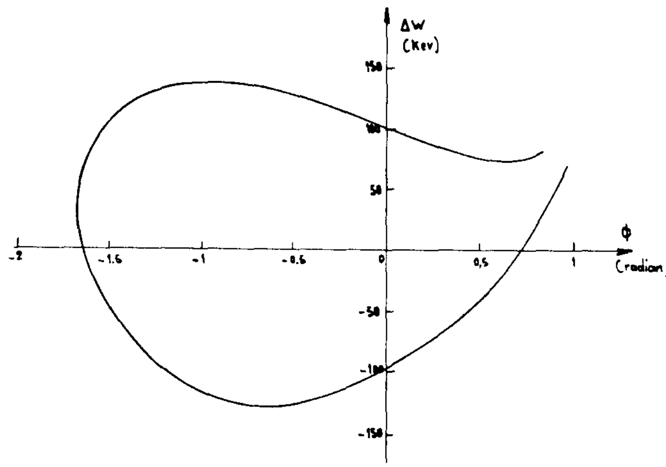


Figure 9.

L cell (cm.)

| | | | | | |
|---|---|---|---|---|---|
| 1 | 6.16 | 21 | 13.52 | 41 | 22.47 |
| 2 | 6.41 | 22 | 13.95 | 42 | 22.94 |
| 3 | 6.72 | 23 | 14.39 | 43 | 23.38 |
| 4 | 7.03 | 24 | 14.82 | 44 | 23.84 |
| 5 | 7.37 | 25 | 15.27 | 45 | 24.29 |
| 6 | 7.70 | 26 | 15.71 | 46 | 24.75 |
| 7 | 8.05 | 27 | 16.15 | 47 | 25.19 |
| 8 | 8.40 | 28 | 16.59 | 48 | 25.65 |
| 9 | 8.76 | 29 | 17.04 | 49 | 26.11 |
| 10 | 9.13 | 30 | 17.50 | 50 | 26.56 |
| 11 | 9.51 | 31 | 17.95 | 51 | 27.01 |
| 12 | 9.88 | 32 | 18.40 | 52 | 27.47 |
| 13 | 10.27 | 33 | 18.85 | 53 | 27.92 |
| 14 | 10.66 | 34 | 19.30 | 54 | 28.37 |
| 15 | 11.06 | 35 | 19.75 | 55 | 28.81 |
| 16 | 11.46 | 36 | 20.20 | 56 | 29.26 |
| 17 | 11.87 | 37 | 20.66 | 57 | 29.69 |
| 18 | 12.27 | 38 | 21.10 | 58 | 30.14 |
| 19 | 12.68 | 39 | 21.57 | 59 | 30.55 |
| 20 | 13.10 | 40 | 22.02 | | |

Figure 10.

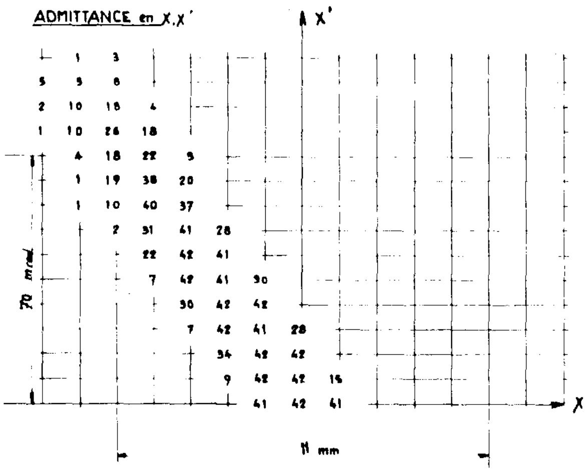


Figure 11.

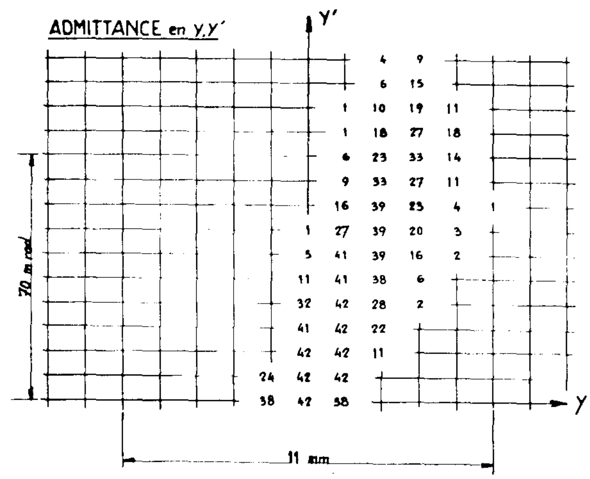


Figure 12.

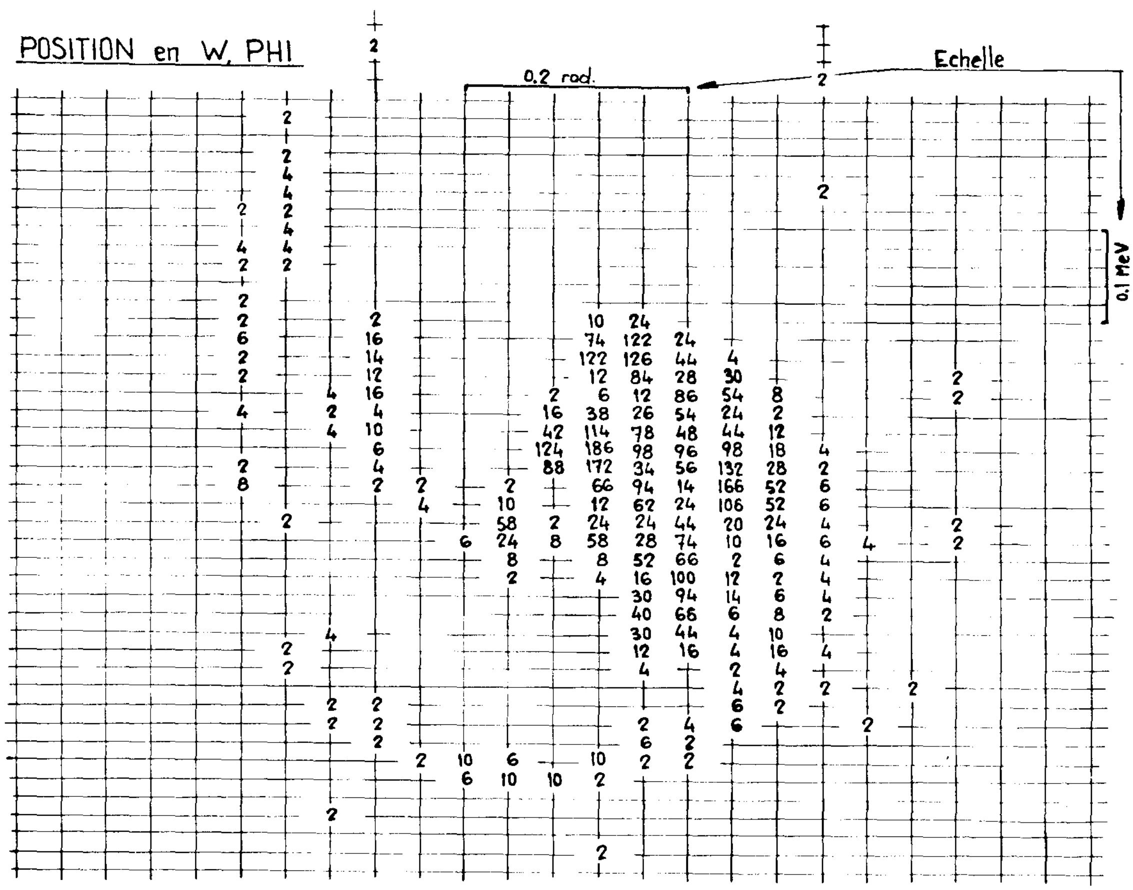


Figure 13.